

## Incoherent Electron Scattering from the Nucleons in Beryllium and Carbon and the Magnetic Size of the Neutron\*†

HANS F. EHRENBERG‡ AND ROBERT HOFSTADTER

*Department of Physics and High-Energy Physics Laboratory, Stanford University, Stanford, California*

(Received December 26, 1957)

The electron scattering at high momentum transfer has been measured from the nucleons in Be, in C, and from the free proton. The data yield the cross section of the average nucleon and of the neutron in relation to that of the proton.  $\sigma_n/\sigma_p(\theta)$  is found to be  $1.16 \pm 0.3$  at 500 Mev and  $135^\circ$ ; it decreases, as expected, for smaller angles and lower energies. If the assumption is made that meson-exchange effects and interactions in the final state are not important, the form factors obtained indicate an apparent root-mean-square radius of the neutron's magnetic-moment distribution of  $(0.53 \pm 0.15) \times 10^{-13}$  cm. It is possible that the apparent small size of the neutron in Be and C is due to the neglect of meson-exchange effects and interactions in the final state. The present result is smaller than a neutron size, given by Yearian and Hofstadter, who compared the cross sections of deuteron and proton and found equal sizes for neutron and proton. If one accepts the latter result, the present experiment can be used to yield a measure of the above neglected effects.

### I. INTRODUCTION

ELECTRON scattering from free protons has been studied previously.<sup>1-3</sup> From the measured cross sections, the electric and magnetic structure of the proton have been determined.<sup>1</sup> It is now of interest to investigate the scattering cross section of the neutron. Since free neutrons are unavailable in sufficiently large densities, it is necessary to use neutrons bound in a light nucleus.

In elastic scattering (from which nuclear sizes may be determined) and in inelastic scattering, in which a nuclear level is excited, the electron is scattered coherently by the nucleus as a whole. In the incoherent scattering to be discussed in this paper, the incident electron is scattered primarily from a single nucleon which recoils and is emitted from the nucleus. Electrons scattered in this process appear in the energy spectrum near the free-proton peak which occurs, for not too small incident energies and scattering angles, at a distinctly smaller energy than the electrons scattered from the whole nucleus. Thus they may easily be distinguished from the latter. Owing to the internal motion of the nucleons, the incoherently scattered electrons have a wide energy distribution, reflecting the momentum distribution of the nucleons. The center of this wide peak is shifted to lower energies with respect to the free-proton peak by an amount corresponding in order of magnitude to the root-mean-square momentum of the various nucleons in the nucleus.

For further details, we may refer to a review article<sup>4</sup> on electron scattering (especially to its Secs. IIIb2, IIIc, and VI), where references to several preliminary measurements of incoherent scattering in deuterium, helium, and beryllium<sup>5</sup> are also reported. We may also call attention to a study of deuterium similar to ours.<sup>6</sup>

At high energies and large angles, that is, for large momentum transfers ( $q$ ), the incoherent scattering is much larger than the combined elastic and inelastic level-scattering from the nucleus because the latter are greatly reduced by finite-size effects.<sup>4</sup> Furthermore, the scattering from individual protons and neutrons at high values of  $q$  is due almost exclusively to their magnetic moments, and the charge scattering from the protons contributes only a small amount. As pointed out previously,<sup>4</sup> the scattering from the neutron would be expected to be about half as large as that of the proton, if the neutron and proton have similar distributions of the density of their magnetic moments. This follows because the scattering is proportional to the square of the magnetic moment at large  $q$  values. On the other hand, a larger neutron cross section would imply either (1) that the magnetic cloud of the neutron is smaller than that of the proton, or (2) that in the special range of  $q$  values studied, because of an unknown complicated structure in the neutron, its form factor has variations leading to larger values than that of the proton. The latter type of behavior could occur if the density distribution goes through a value of zero at a distance at which the experiments have a high sensitivity.

It was the purpose of this work to study the incoherent electron scattering from beryllium in order to determine the cross section of the neutron. Some time

\* The research reported here was supported jointly by the Office of Naval Research and the U. S. Atomic Energy Commission, and by the U. S. Air Force, through the Office of Scientific Research of the Air Research and Development Command.

† Presented at the Heidelberg Meeting of the German Physical Society, September, 1957 (unpublished).

‡ On leave of absence from Physikalisches Institut der Universität Bonn.

<sup>1</sup> R. Hofstadter and R. W. McAllister, *Phys. Rev.* **98**, 217 (1955).

<sup>2</sup> R. W. McAllister and R. Hofstadter, *Phys. Rev.* **102**, 851 (1956).

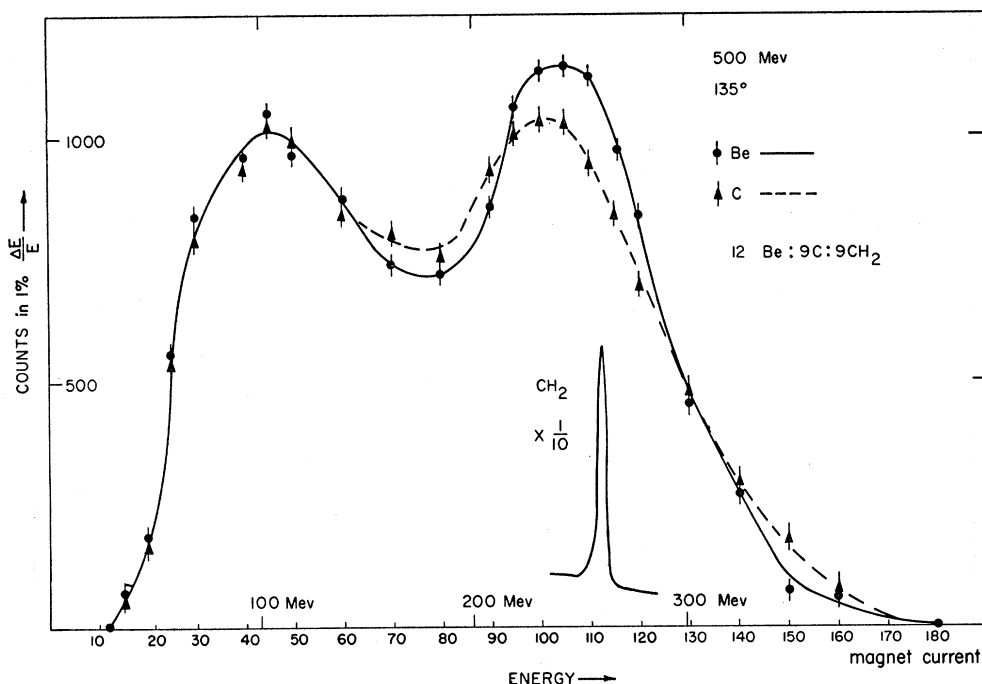
<sup>3</sup> E. E. Chambers and R. Hofstadter, *Phys. Rev.* **103**, 1454 (1956).

<sup>4</sup> R. Hofstadter, *Revs. Modern Phys.* **28**, 214 (1956).

<sup>5</sup> E. E. Chambers and R. Hofstadter (unpublished); see also reference 4 and *Proceedings of the Seventh Annual Rochester Conference on High-Energy Nuclear Physics, 1957* (Interscience Publishers, Inc., New York, 1957).

<sup>6</sup> M. R. Yearian and R. Hofstadter, *Phys. Rev.* **110**, 552 (1958) this issue.

Fig. 1. Energy spectrum of the incoherently-scattered electrons of 500-Mev incident energy at  $135^\circ$  from the nucleons in Be and C. Both targets have equal numbers of nucleons per  $\text{cm}^2$ . The ordinate gives counts per  $1.065 \times 10^{24}$  nucleons/ $\text{cm}^2$ , per  $3.75 \times 10^{15}$  incident electrons ( $= 600$  microcoulombs), per solid angle  $4.95 \times 10^{-3}$  and per 1% energy interval. The second peak on the low-energy side is caused by electrons which have produced pions in their scattering process. The polyethylene peak is given in a scale corresponding to the same carbon content as in the carbon target.



ago, Chambers and Hofstadter<sup>5</sup> made a preliminary examination of that nucleus, which shows that the method is feasible with beryllium, where there is a well-known loosely-bound neutron. The cross section corresponding to this neutron might be expected to show up at the peak of the incoherent continuum. The idea was then to determine the scattering cross section of the neutron as the difference between the values for Be<sup>9</sup> and "Be<sup>8</sup>." If the scattering is truly incoherent, "Be<sup>8</sup>" can be considered to be  $\frac{2}{3}$  of the C<sup>12</sup> nucleus.

In the foregoing we have implicitly made the assumption that meson-exchange effects do not contribute appreciably to the area under the inelastic Be and C peaks. While real meson production is observed in the left-hand peak of Fig. 1, virtual meson production and meson exchange may add to the area under the right-hand peak. We will discuss this problem later (Sec. IV).

## II. APPARATUS AND EXPERIMENTAL METHOD

This experiment has been performed with the Stanford linear accelerator as the source of electrons, by using the standard arrangement described in reference 4, Sec. IVb. The incident electron beam was analyzed magnetically so that the energy band was 1% wide. The electron current was measured by a large Faraday cup placed behind the target and integrated by a vibrating-reed electrometer with a feedback arrangement. Beam currents up to a maximum value of  $4 \times 10^{10}$  electrons per pulse ( $= 4 \times 10^{-7}$  amp) were used (60 pulses per second).

The targets of Be and C (graphite) were plates of equal weight/ $\text{cm}^2$ , namely,  $683 \text{ mg}/\text{cm}^2 = 408 \times 10^{21}$  nucleons/ $\text{cm}^2$ . The comparison proton peak was meas-

ured in a polyethylene plate. A CsBr crystal was used as before to adjust the position and shape of the beam spot. The targets could easily be replaced by each other with the beam spot remaining fixed. In all cases the target angle was set at half the scattering angle.

The scattered electrons were analyzed by the 36-in. double-focusing magnetic spectrometer<sup>3,4</sup> and counted in a standard manner with a fluorocarbon Čerenkov counter (index of refraction = 1.27). The energy acceptance slit was made 1% wide and the angular aperture was approximately  $2^\circ$  in the plane of the beam and  $8^\circ$  in the perpendicular plane. As has already been discussed in reference 4, the use of this Čerenkov counter, in connection with the discriminator setting high enough, eliminates meson counting, and a confirmation of this fact comes from the absence of counts when the spectrometer current is reversed. In the latter case, positive mesons would have been detected in approximately equal numbers compared to the negative mesons accompanying the scattered electrons.

In order to increase the accuracy of comparison, the data from Be and C were taken alternately at each spectrometer setting. In almost every run at least one free-proton peak from the polyethylene target was taken, and the carbon background could easily be subtracted by using the measured data in carbon. We made no special attempt to determine absolute values of the cross sections, since we related all our results to the proton cross section. The relative cross sections, obtained for the free proton at different angles and energies, are in good agreement with Chambers and Hofstadter.<sup>3</sup> The absolute value is somewhat less than that calculated in their work. The reason for this has

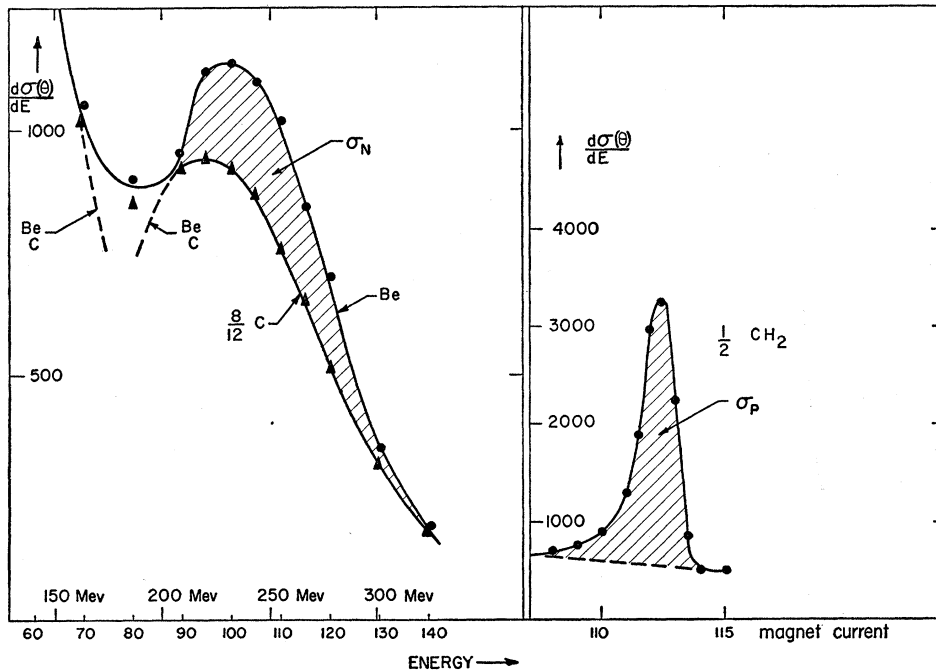


FIG. 2. Differential cross section for the Be nucleus, for  $8/12$  of the C nucleus, and for the free proton. The units of  $d\sigma(\theta)/dE$  are  $1.96 \times 10^{-37}$  cm<sup>2</sup>/Mev sterad. The area between the Be and the C curve represents the cross section of one neutron in Be.  $\sigma_n/\sigma_p$  is found to be 1.16.

not been investigated, but is probably connected with the high bias setting of the discrimination mentioned above.

### III. RESULTS

#### (a) 500 Mev, 135°

Figure 1 shows the energy distribution of the 500-Mev electrons scattered at 135°. These data form the main object of the experiment. The peak on the right represents the electrons scattered incoherently from the nucleons, while the peak to the left represents those electrons that have scattered while producing mesons and consequently have lower energy.<sup>4</sup>

The incoherent peak to the right is the one that will interest us in these experiments. This peak has been measured on several occasions with good statistics. The absolute counting rates were reproducible to within 6%, and the relative values between Be, C, and CH<sub>2</sub> agreed with each other to better than 2%.

In this figure we see clearly the shift of the maximum in relation to the free-proton peak. The shift is somewhat larger for C than for Be. Furthermore, one notices that the momentum distribution of the nucleons in C is slightly broader than in Be. These features are also observed in the measurements taken at smaller angles and lower energies.

The data in Fig. 1 were converted into counts per constant-energy interval by use of the spectrometer calibration and its dispersion characteristic. This correction is the familiar  $1/E$  correction. In the curves thus corrected, the area under each peak (Be, C,  $p$ ) represents the corresponding cross section, and from comparison of the areas we may obtain the cross section

per nucleon (averaged over protons and neutrons) in Be and C, in relation to the cross section of the free proton. Unfortunately, there is superposed on the incoherent peak the tail of the meson-producing electron peak. Thus the left-hand side of the incoherent peak is not accurately known. Because of the spatial symmetry of the momentum distributions of the nucleons, half of the nucleons contribute to each half of the peak. We may take the area to the right of the center line and relate it to one-half of all nucleons in the target. The result obtained is  $(\sigma_{inel})_{Av} = 1.08 \pm 0.1$ , in Be and  $(\sigma_{inel})_{Av} = 1.17 \pm 0.1$ , in C.

The relative cross section for  $\sigma_p$  is taken to be 15.8% larger than the area shown in the right-hand side of Fig. 2. This correction accounts for the number of electrons not counted in the proton peak due to the radiative losses (Schwinger correction and straggling effects). The amount lost in the proton peak due to these causes is 25%, and the amount lost in the Be and C peaks is 8% in each case.

Since this determination of the area depends sensitively upon where one places the center line, we also took the area after shifting the center line far over to the right (actually to the position where the maximum appears when we omit the  $1/E$  correction), and we obtained values of 0.82 and 0.96 for  $(\sigma_{inel})_{Av}$  in Be and C, respectively. We believe that this is even less than a lowest possible limit, when we allow for quite a large distortion of the incoherent peak by the meson-production peak and for other effects, which might tend to falsify the true position of the center of the incoherent peak.

By relating the measured incoherent-scattering cross

sections of Be and C nuclei to the average nucleon, we have not made any special assumption about the particular nucleons in the nucleus. If we now make the assumption that the momentum transfer is high enough so that the nucleons may be treated as free and independent particles, we can interpret these results in terms of individual proton and neutron cross sections. This will be done in the discussion in the next section.

Under this assumption we can now make a second and independent evaluation of the data, which follows the procedure outlined in the introduction, and determine the cross section of the neutron in a differential method between Be and C. This means that we shall take the difference between Be and  $\frac{2}{3}$  of C<sup>12</sup>. Figure 2 shows this comparison between the experimental Be and C data after the spectrometer correction has been made and after the C data have been multiplied by 8/9. This factor corresponds to 8/12 in the number of atoms. The area between both curves gives the cross section of one neutron in Be. By comparison with the free-proton peak, we obtain

$$\sigma_n/\sigma_p = 1.16 \pm 0.1.$$

We may emphasize that this method is less affected by distortion from the meson-production peak than is the determination of the whole area for Be and C separately. Also the need for systematic corrections is greatly reduced.

Still another variation may be used as a third method, wherein we obtain the difference between the Be curve and the unreduced C curve (i.e., for equal numbers of nucleons) and calculate in this way

$$\sigma_n - \sigma_p = (0.00 \pm 0.1)\sigma_p; \text{ thus } \sigma_n = (1.00 \pm 0.1)\sigma_p.$$

Each of the three methods described gives a somewhat different value for  $\sigma_n/\sigma_p$  because of the different ways in which the differences in shape and position between the Be and C curves influence the results. As a weighted average, we will take the value

$$\sigma_n/\sigma_p = 1.17 \pm 0.3 \text{ for } 500 \text{ Mev and } 135^\circ,$$

with a limit of error that we consider safe with respect to most kinds of possible systematic errors resulting from distortion by the meson-production peak and to the differences in the momentum distribution. The limits of errors also include the corrections which ought to be made for theoretical reasons (see below). The latter fortunately are not large, at high  $q$  values, and some of them tend to cancel each other.

The main effects of the corrections of the cross section are: (1) the center of the incoherent peak occurs at a lower energy than the free-proton peak, because the nucleon is bound and has a slightly lower "effective mass" in the kinematics of the scattering process, and (2) the moving nucleons with different momentum directions contribute differently to the total cross section, since energy and scattering angle in the center-

of-mass system of each collision are different, depending upon the momentum of the nucleon.

Since *magnetic* scattering from point nucleons is nearly independent of energy and angle, and since the charge scattering is small for high  $q$  at large angles, the main part of the correction in each case comes from the change of the form factor with  $q$ . The  $q$  value for the center of the Be peak is 3% smaller than for the free proton; thus the form factor  $F^2$  and the cross section are about 6% larger. Since in our calculations we used only the nucleons on the high-energy side of the center-of-peak, which is closer to the proton peak, we have already implicitly accounted for a large part of this correction. Regarding the effect of the moving nucleons, we may note that all nucleons on the right-hand side of the center line have a momentum component towards the electron. Therefore, their cross sections are slightly smaller than for nucleons at rest. In this sense our cross section is too small by a few percent. An accurate consideration of all these effects could be done by superposing the differential cross sections calculated for each moving nucleon in the corresponding center-of-momentum frame. Because of larger experimental uncertainties, it is not worth while to make those corrections in our data. For the differential Be- $\frac{2}{3}$ C method, these corrections are even smaller, since the area corresponding to the single neutron is located at a position very close to the proton peak.

### (b) Other Energies and Angles

As a check of the above-described work, we may employ a kind of counter-example which should be useful in understanding the results. At lower energies and smaller angles, the charge scattering becomes much larger than the magnetic scattering. Hence, at such values of  $q$ , the scattering cross section should be dominated by the scattering from the protons alone. Unfortunately, the test cannot be made uniquely, since, at the small  $q$  values, the incoherent scattering disappears because the different nucleons cannot be treated as independent. Moreover, there is the experimental difficulty that the elastic- and inelastic-level scattering peaks are also very large in comparison to the remaining small incoherent peak. However, it is possible to carry out some experiments in the intermediate region, where the magnetic scattering still contributes a fair amount, but less than at 500 Mev and 135°.

For example, in Fig. 3, we show curves for 400 Mev and 90°. The meson-production peak decreases quite noticeably as one goes to smaller angles. This is one favorable aspect of these experiments. The results of this, as well as of a set of later measurements under different conditions, are shown in Fig. 4. The evaluation of the data was made in the manner described for 500 Mev and 135°. The cross section of the average nucleon shows the expected decrease of the neutron's contribution as we go towards lower energies and smaller

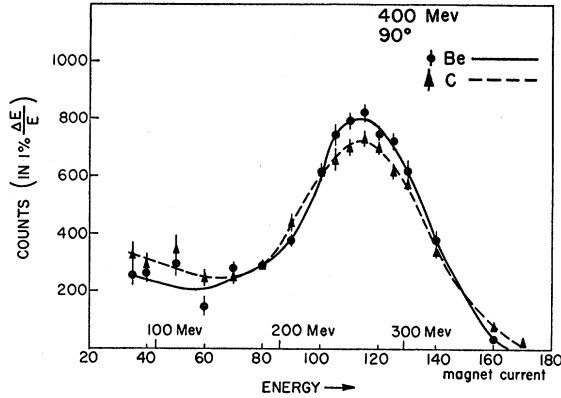


FIG. 3. Energy spectrum of the incoherent electron scattering at 400 Mev,  $90^\circ$ . Compared to Fig. 1, the decrease of the meson-production peak may be noticed.

angles, where it approaches the value given by the protons alone. The accuracy of the smaller-angle measurements is, in general, not good enough to make effective use of the differential Be- $\frac{2}{3}$ C method, although in a few cases the agreement is satisfactory.

In the following discussion we shall tentatively make the assumption that meson-exchange effects add only very small amounts to the inelastic peaks. We shall later discuss what happens if this assumption is not made.

#### IV. DISCUSSION AND CONCLUSIONS

The cross section of the proton (mass  $M$ , Dirac moment 1, Pauli moment  $\kappa$ ) and likewise of the neutron, for scattering of electrons of the incident energy  $E$  at the angle  $\theta$  (in the laboratory frame), is given by Rosenbluth's<sup>7</sup> formula, which we may write here in the following form:

$$\sigma = \left( \frac{e^2}{Mc^2} \right)^2 \frac{1}{[1 + (2E/Mc^2) \sin^2(\theta/2)]^2} \left\{ \frac{1}{[2 \tan(\theta/2)]^2} \times \left[ \left( \frac{2Mc}{\hbar q} \right)^2 F_1^2 + \kappa^2 F_2^2 \right] + \frac{1}{2} [F_1 + \kappa F_2]^2 \right\},$$

where

$$\hbar^2 q^2 = \frac{[2(E/c) \sin(\theta/2)]^2}{1 + (2E/Mc^2) \sin^2(\theta/2)}$$

means the square of the momentum transfer of the electron in the scattering process. The form factors  $F_1$  and  $F_2$ , both functions of  $q^2$ , take into account the finite size of both the Dirac and the Pauli magnetic-moment distributions. (As regards the exact meaning of  $F_1$  and  $F_2$  and their relation to the electric and magnetic density of the nucleon's structure, see Yennie, Lévy, and Ravenhall.<sup>8</sup>)

<sup>7</sup> M. Rosenbluth, Phys. Rev. **79**, 615 (1950).

<sup>8</sup> Yennie, Lévy, and Ravenhall, Revs. Modern Phys. **29**, 144 (1957).

In the static limit, i.e., for  $q=0$ , when proton and neutron can be considered as point particles, the form factors have the values  $F_{1p}(0)=F_{2p}(0)=F_{2n}(0)=1$  and  $F_{1n}(0)=0$ . (Here and in the following equations the indices  $p$  and  $n$  refer to proton and neutron, respectively.) Thus the ratio of the cross sections for point proton and point neutron is

$$\left( \frac{\sigma_n}{\sigma_p} \right)_{\text{point}} = \frac{\kappa_n^2 [1 + \frac{1}{2} \cot^2(\theta/2)]}{\frac{1}{2} \cot^2(\theta/2) [(2Mc/\hbar q)^2 + \kappa_p^2] + (1 + \kappa_p)^2} = A(\theta, q).$$

For the interpretation of the experiments, we shall introduce, as usual, "total form factors," defined by  $\sigma_{p,n} = (F_{p,n})^2 \times (\sigma_{p,n})_{\text{point}}$  so that

$$\sigma_n/\sigma_p = (F_n^2/F_p^2) \times A(\theta, q).$$

From the measured cross section  $\sigma_n/\sigma_p = 1.17 \pm 0.3$ , we may calculate  $F_n^2/F_p^2 = 2.6 \pm 0.6$  at 500 Mev,  $135^\circ$ . Using the known proton form factor,<sup>1-4</sup> we obtain for the neutron

$$F_n^2 = 0.39 \pm 0.1 \quad \text{at} \quad q^2 = 11.5 \times 10^{26} \text{ cm}^{-2}.$$

We may now turn back to Fig. 4, where the cross section of the average nucleon is plotted as a function of  $A$ . Under the assumption that the nucleons scatter

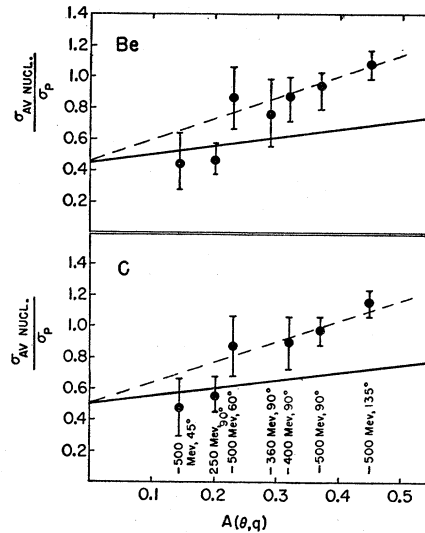


FIG. 4. Experimental cross section per nucleon in Be and in C, in units of the free-proton cross section for several experimental conditions. The data are arranged along an abscissa which is chosen for convenience and contains the experimental conditions  $\theta$  and  $q$  in such a way that  $A(\theta, q)$  is the ratio of  $\sigma_n/\sigma_p$  for point particles. The heavy lines indicate the cross section of the average nucleon as a function of  $A$  in the case that the neutron has the same magnetic form factor as the proton. (This coincides with the case of point particles and shows that, for  $A=0$ , the average nucleon cross section is  $4/9$  for Be and  $6/12$  for C.) The dotted lines through the experimental points correspond to a (form factor)<sup>2</sup> of the neutron = 2.4 (in Be) and 3.0 (in C) times that of the proton. The errors in this figure refer to the observational accuracy of the measurements.

as independent particles, we obtain

$$\begin{aligned} \frac{\sigma_{Av \text{ nucleon}}}{\sigma_p} &= \frac{1}{9} \left( 4 + 5 \frac{F_n^2}{F_p^2} \times A \right) \text{ in Be} \\ &= \frac{1}{12} \left( 6 + 6 \frac{F_n^2}{F_p^2} \times A \right) \text{ in C.} \end{aligned}$$

The heavily-drawn straight line in each part of the figure refers to the case  $F_n = F_p$ . The experimental points at large  $A$  clearly fall above this line, thus indicating  $F_n > F_p$ . The slope of the dotted line corresponds to  $F_n^2/F_p^2 = 2.4$  in Be and  $= 3.0$  in C. (The dotted lines do not, of course, imply that we believe that  $F_n/F_p$  is constant at all  $A$  values.)

The (form factors)<sup>2</sup> obtained for the neutron are shown in Fig. 5 as functions of  $q^2$ . The  $F_n$  for low  $q$  cannot be given with any accuracy, since the experiments at small  $A$  are very insensitive to the cross section of the neutron. However, the large values of the form factor are very persistent, and this may be some indication that the magnetic form factor at low  $q$  is in the neighborhood of unity or slightly higher, as might be given by a density distribution which changes sign as a function of radial distance. We may note that an analysis of the preliminary data of Chambers and Hofstadter<sup>5</sup> at 600 Mev and 135° gives a value of  $\sigma_n/\sigma_p = 1.0 \pm 0.3$ .

The present data are certainly not sufficient to make a structural analysis of the neutron as has been made in the case of the proton.<sup>1-4</sup> There,  $F_{1p}(q)$  and  $F_{2p}(q)$  were evaluated separately from the experimental "total form factor" and turned out to be nearly identical. The root-mean-square radius was found to be  $0.77 \times 10^{-13}$  cm for each of the two distributions.

For the neutron not only is  $F_{1n}(q=0) = 0$  (zero total charge), but from the experiments on scattering of neutrons by atoms<sup>9</sup> it is known that the coefficient of  $q^2$ , in an expansion of  $F_{1n}(q^2)$  in powers of  $q^2$ , is also close to zero. That makes it most probable that the "total form factor"  $F_n$ , obtained in our experiments, is the  $F_{2n}$  in the Rosenbluth formula and that we can thus place  $F_{1n} \equiv 0$ . (A large coefficient of  $q^4$  in  $F_{1n}$  would involve quite a complicated charge distribution in the neutron.)

With the above assumptions, we can state that the magnetic distribution in the neutron is apparently more confined than in the proton but not so confined as to be a point (see Fig. 5). For the rms radius of a bound neutron we obtain

$$\langle r_{2n} \rangle = (0.53 \pm 0.15) \times 10^{-13} \text{ cm.}$$

This result is nearly independent of the special structural model chosen for transforming the form factor

<sup>9</sup> See references 11 and 12 in reference 8.

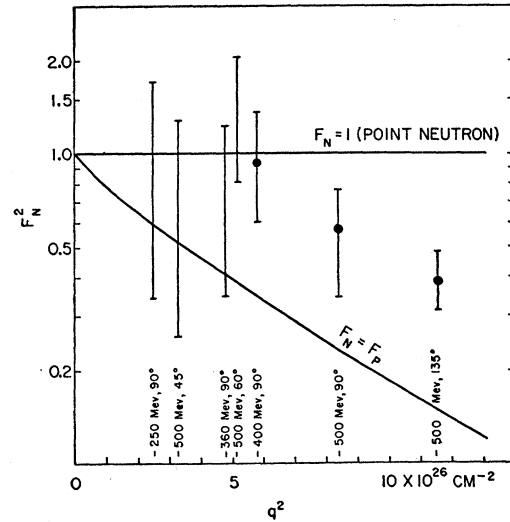


FIG. 5. Experimental (form factor)<sup>2</sup> of the neutron as a function of the square of the momentum transfer. At large  $q$  values, the form factor of the neutron is 2.6 times larger than that of the proton. The limits of error given include all possible systematic errors in the experiments. At low  $q$  values, the experiments are not able, for essential reasons, to yield information on the neutron cross section with any accuracy. The root-mean-square radius of the magnetic-moment distribution of the neutron is about  $(0.53 \pm 0.15) \times 10^{-13}$  cm, if the density distribution is monotonic.

into  $\langle r_{2n} \rangle$ ; as long as we assume that the distribution is monotonic. There appears to be little doubt that the bound neutron and proton are different in size or shape if the simple assumptions we have made, such as neglecting meson exchange, prove to be justified.

However, since we have compared the cross sections of bound nucleons with that of the free proton, we are, of course, making the special assumption that the internal structures of neutron and proton are not affected by the fact that they are bound in a nucleus and thus are under the influence of the nuclear forces. Moreover, we have made the assumption that meson-exchange effects are unimportant. We may judge how well this assumption holds by the comparison of these results with those in the deuteron,<sup>6</sup> where the neutron and proton are under the influence of the strong nuclear force only a small fraction of the time and where the neutron size is essentially equal to that of a free proton.

It may thus be pointed out that the real use of experiments such as this one will probably be to tell what happens to the neutron when it is bound within a nucleus as compared with its free behavior. When related to the deuteron results, we may say that there are probably meson-exchange effects in Be and C and that these account for the apparently smaller neutron size.

#### ACKNOWLEDGMENTS

We wish to express our thanks to the operating crew of the Stanford linear accelerator and to all members

of the electron-scattering group for their continued help in setting up the experiments, as well as for discussions on experimental and theoretical questions. We also wish to thank Dr. D. G. Ravenhall and Mr.

R. Blankenbecler for valuable discussions. One of the authors (H. F. E.) is grateful to the Deutsche Forschungsgemeinschaft for the grant of a stipend which permitted him to stay at Stanford for one year.

## Method for Determining the $K_+^0 - K_-^0$ Mass Difference\*

MYRON L. GOOD

Radiation Laboratory, University of California, Berkeley, California

(Received October 28, 1957)

The equations of motion for the amplitudes of short-lived ( $K_+^0$ ) and long-lived ( $K_-^0$ ) neutral  $K$  mesons in an absorber are simplified for the case of dominance of the decay term. For the case of a thick absorber, a simple relation between the intensities of scattered and unscattered regenerated  $K_+^0$ , at zero degrees, results; the relation is sensitive to the  $K_+^0 - K_-^0$  mass difference.

THE phenomenon of regeneration of the short-lived neutral  $K$  meson in a beam of long-lived neutral  $K$ 's is a crucial test of the particle-mixture hypothesis of Gell-Mann and Pais<sup>1</sup>; what we wish to show here is that it also permits a rather direct determination of the difference in mass of the two particles.

The process has been studied theoretically<sup>2,3</sup>; preliminary experimental verification of the basic ideas involved has been obtained by Lederman *et al.*<sup>4</sup> and by Fowler, Lander, and Powell,<sup>5</sup> and others.

The theory of the process is independent of the questions of whether or not charge conjugation ( $C$ ), parity ( $P$ ), or time reversal ( $T$ ) are valid symmetry operations.<sup>6,3</sup>

For the short-lived and long-lived particles, respectively, we adopt, following Lee and Yang, the names  $K_+^0$  and  $K_-^0$ . Otherwise the notation used is that of reference 3.

First, we observe that, in most, if not all, circumstances  $K_+^0$  decay predominates over absorption processes, so that it is a good approximation to set

$$\beta ck \left| \frac{n-n'}{2} \right| \ll \frac{1}{2\gamma\tau_+}.$$

(This is precisely what makes the regeneration so small.<sup>2</sup>) With this approximation, the solutions for the amplitudes ( $\alpha_+, \alpha_-$ ) of  $K_+^0, K_-^0$  in the absorber simplify

considerably:

$$\begin{pmatrix} \alpha_+(t) \\ \alpha_-(t) \end{pmatrix} \simeq \begin{bmatrix} -\left(\frac{R}{R^2}\right) e^{-(i\omega_+ + 1/2\gamma\tau_+)t} \\ \left(\frac{R}{1}\right) e^{-i\omega_- t} \end{bmatrix} e^{\frac{1}{2}\beta ck(n+n')t}, \quad (1)$$

where

$$R \simeq \frac{\beta\gamma ck(n-n')}{2[(1/2\tau_+) + i(\omega_+^0 - \omega_-^0)]}, \quad \text{and} \quad |R| \ll 1.$$

The initial conditions have been taken as  $\alpha_+(0)=0$ ,  $\alpha_-(0)=1$ , and  $1/\tau_-$  has been neglected in comparison with  $1/\tau_+$ . If we now confine ourselves to thicknesses ( $L$ ) large compared with the  $K_+^0$  decay distance, we can drop the first term, and we have, for the  $K_+^0$  intensity emerging from the absorber,

$$|\alpha_+(L)|^2 \simeq |R|^2 e^{-\frac{1}{2}N(\sigma+\sigma')L}. \quad (2)$$

This refers to the unscattered regenerated  $K_+^0$ . The  $K_+^0$  intensity regenerated by scattering through an angle  $\phi$  at depth  $x$  is, in the same spirit (evaluated at  $\phi=0$ ),

$$\left| \left( \frac{dI_s}{dx} \right) dx d\Omega \right|_{\phi=0} \simeq \frac{k^4}{16\pi^2 N} |n-n'|^2 dx d\Omega e^{-\frac{1}{2}N(\sigma+\sigma')x}. \quad (3)$$

To evaluate the scattered  $K_+^0$  intensity emerging from the absorber at  $\phi=0$ , we must multiply Eq. (3) by the probability of escape of the regenerated  $K_+^0$  without decay or further scattering, and must integrate with respect to  $x$ . (This gives the contribution of single scattering. The particles scattered as  $K_-^0$  can of course, rescatter into  $K_+^0$ , and so on. Thus double and higher-order scatters can contribute also. For the time being, we consider only single scattering.) The scattered  $K_+^0$ , being incoherent with the incident beam, decays with essentially the exponent of the first term of Eq. (1),

\* This work was done under the auspices of the U. S. Atomic Energy Commission.

<sup>1</sup> M. Gell-Mann and A. Pais, Phys. Rev. **97**, 1387 (1955).

<sup>2</sup> K. Case, Phys. Rev. **103**, 1449 (1956).

<sup>3</sup> M. L. Good, Phys. Rev. **106**, 591 (1957).

<sup>4</sup> Lande, Lederman, and Chinowsky, Phys. Rev. **105**, 1925 (1957).

<sup>5</sup> Fowler, Lander, and Powell, Bull. Am. Phys. Soc. Ser. II, **2**, 236 (1957).

<sup>6</sup> Lee, Yang, and Oehme, Phys. Rev. **106**, 340 (1957).